Astron. Astrophys. 334, 253–263 (1998)

ASTRONOMY AND ASTROPHYSICS

Progressive dispersal of the dense gas in the environment of early-type and late-type Herbig Ae-Be stars

A. Fuente[1], **J. Martín-Pintado**[1], **R. Bachiller**[1], **R. Neri**[2], **and F. Palla**[3]

[1] Observatorio Astronómico Nacional (IGN), Campus Universitario, Apdo. 1143, E-28800 Alcalá de Henares (Madrid), Spain
[2] Institut de Radioastronomie Millimétrique (IRAM), 300 rue de la Piscine, Domaine Universitaire, F-38406 St Martin d'Hères Cedex, France
[3] Osservatorio Astrofisico di Arcetri, Largo Enrico Fermi 5, I-50125 Firenze, Italy

Received 18 December 1997 / Accepted 18 February 1998

Abstract. We have carried out a systematic study of the environment of 14 Herbig Ae/Be (HAEBE) stars at millimeter wavelengths. Our data show that there is a progressive dispersal of the dense gas associated with these stars in their evolution to the main sequence. The efficiency of this dispersal is very different for "early-type" (B0-B5) and "late-type" (B5-A5) stars. While in early-type stars the mean gas density in a radius of 0.08 pc decreases by almost two orders of magnitude during their evolution to the main sequence, in late-type stars it decreases by less than an order of magnitude. Because of this different efficiency, there is no correlation between the ages of the stars and the Hillenbrands' infrared (IR) groups. Early-type stars evolve from the Hillenbrand's Group I to Group III in their way to the main sequence, while late-type stars evolve from Group II to Group I.

Since the morphology of the parent molecular cloud seems to be strongly dependent on the age of the stars, we propose a new classification for both, early-type and late-type HAEBE stars. We refer as Type I stars to those immersed in a dense clump. These stars are associated with bipolar outflows and have ages $\sim 10^5$ yrs. We call Type III stars those that have completely dispersed the surrounding dense gas and are located in a cavity of the molecular cloud. Bipolar outflows are not associated with them and their ages are $> 10^6$ yrs. Type II stars represent the intermediate case, they are immersed in the molecular cloud but they are not at the peak of a dense clump. The advantage of this new classification is that it allows a simple and easy estimate of the evolutionary stage and age of HAEBE stars.

Key words: stars: formation – radio-lines: ISM – stars: pre-main sequence – ISM: abundances – ISM: clouds – ISM: molecules

1. Introduction

Although Herbig Ae/Be (HAEBE) stars were identified more than 30 years ago as the higher mass counterpart of T Tauri stars (Herbig 1960), their origin and evolution remain largely unknown nowadays. In fact, a big observational and theoretical effort has been devoted to low mass stars during these last 30 years, but only few studies (mainly in the course of the last 10 years) have been aimed to understand the pre-main sequence evolution of stars with intermediate masses. Such studies have provided at least two important conclusions: 1) Although HAEBE stars share spectroscopic and photometric properties with T Tauri stars, important differences exist between low and intermediate mass stars (Finkezeller 1985, Herbst et al 1982, Natta et al. 1993); 2) HAEBE stars constitute a much more heterogeneous group than T Tauri stars.

Hillenbrand et al. (1992) studied the spectral energy distribution of 47 Herbig Ae-Be stars and classified them according to their IR spectral index in three IR groups, Group I, II and III. Group I corresponds to the stars whose infrared excess can be well fitted assuming that the IR excess emission arises from a flat circumstellar accretion disk. Group II corresponds to objects which are best interpreted as star/disk systems surrounded by gas and dust which is not confined to a disk. Finally, stars with small infrared excess belong to Group III. This classification represents an evolutionary sequence characterized by a progressive decrease of the amount of circumstellar material from Group II $\rightarrow$ Group I $\rightarrow$ Group III. However, such a classification is based on infrared continuum observations, which only trace the warm dust very close to the star and could suffer from important opacity effects in these regions.

To improve our knowledge on the evolution of HAEBE stars we have carried out a systematic study of the environment of these stars in molecular lines and continuum emission at millimeter (mm) wavelengths. Very little is known on the morphology and density structure of the gas surrounding HAEBE stars. Although dense clumps have been found associated with some of them, recent observational studies reveal that other HAEBE stars are located in a cavity of the molecular cloud that is spatially coincident with the optical nebulosity (Fuente et al. 1993, Hillenbrand 1995, Fuente et al. 1996). Whether this cavity is the consequence of the photodissociation of the molecular material by the stellar UV radiation and/or the result of the dispersal of the dense material by the mass-loss phenomena associated with young stars is still an unresolved problem. The morphology and density structure of the dust surrounding these stars are also poorly known. In contrast to continuum IR emission, the continuum emission at millimeter wavelengths is expected to be optically thin and trace dust as cool as $T_d \sim$ 10 K. But

just a few works have been done in this range (Natta et al. 1997, Di Francesco et al. 1997, Henning et al. 1994, Mannings 1994, Reipurth et al. 1993). Furthermore, most of them consist of observations only toward the star position, and do not provide much information on the spatial distribution and density structure of the dust in the surroundings of HAEBE stars.

2. Selected sample

To investigate the evolutionary stage of these stars on the basis of the morphology, spatial distribution and density structure of the gas and dust surrounding them, we have selected a sample of 14 HAEBE stars with different infrared spectral energy distributions (SEDs): 6 belong to Group I, 6 to Group II and 2 to Group III. It is known that some properties associated with young stars are strongly dependent on their spectral type. In fact, Testi et al. (1997) concluded that clustering is significant only for stars of spectral type earlier than B7. Skinner et al. (1993) found that there is a lack of detections of continuum emission at 3.6 cm for stars with spectral type later than A0. The variability of photometric properties and the association with H_2O masers are also dependent on the spectral type (Finkezeller & Mundt 1984, Palla & Prusti 1993). To investigate the possible dependence of the structure of the dense material around HAEBE stars on the stellar spectral type, we were careful that our sample included stars of different spectral types, and hence, of different masses. In fact, our sample includes 6 stars with spectral types B0-5 (masses $\gtrsim$ 6 $M_\odot$) and 8 stars with spectral type later than B5 (masses $\lesssim$ 6 $M_\odot$). Hereafter we will refer to these groups as "early-type" and "late-type" HAEBE stars respectively. To achieve a uniform spatial scale, we have selected stars at a similar distance (d $\sim$ 500-1300 pc). The selected objects and the main stellar parameters are listed in Table 1.

3. Observations

We have mapped a region of $\approx 4' \times 4'$ around 11 stars of our sample in the ^{13}CO 1$\rightarrow$0 and CS 3$\rightarrow$2 molecular lines and in the continuum emission at 1.3mm. In addition, we have observed HK Ori in mm-continuum emission, BD 61154 in the ^{13}CO 1$\rightarrow$0 and CS 3$\rightarrow$2 lines and HD 200775 in the ^{13}CO 1$\rightarrow$0 line. We decided to observe the vicinity of these stars in the J=1$\rightarrow$0 line of ^{13}CO because this is a very good tracer of the molecular column density in a wide range of visual extinctions. In addition, the J=3$\rightarrow$2 line of CS was chosen because it is sensitive to the relatively high densities present in star forming regions. Finally, mm continuum observations allow a direct estimate of the mass of the circumstellar dust.

3.1. Molecular line observations

The observations of the molecular lines were carried out in 1996, July with the IRAM 30m telescope on Pico de Veleta (near Granada, Spain). Both transitions were observed simultaneously with the SIS receivers. Forward efficiency, main beam efficiency, and typical system temperature were 0.92, 0.68, and 350 K at 3mm and 0.90, 0.52, and 500 K at 2 mm. The Half Power Beam Width of the telescope is $24''$ at the frequency of the ^{13}CO 1$\rightarrow$0 line and $16''$ at the frequency of the CS 3$\rightarrow$2 line. The line intensities are given in units of main beam temperature. Both transitions were observed with a spectral resolution of $\sim$ 78 kHz using an autocorrelator split in several parts. Maps of $\sim$ 1 pc $\times$ 1 pc ($\approx 200'' \times 200''$ at a distance of 1000 pc) with a spacing of $20''$ were carried out toward each star. In the case of HD 52721 only a cross of 15 points centered on the star was observed since no emission was detected at any position.

3.2. 1.3mm continuum

The 1.3mm continuum data were obtained during 1997 February 11-20 using the MPIfR 19-channel bolometer array installed at the IRAM 30m telescope. The observations were carried out in the so-called on-the-fly mode and for the most part two coverages were obtained for each of the targets. The typical map size was $240'' \times 220''$, the effective resolution about $10'' - 11''$ and the sensitivities were between 3.5 and 10 mJy/beam. During the observing sessions we employed an azimuthal wobbler throw of $41''$ switched at a rate of 2 Hz. Pointing, focus, skydips and calibrations maps were obtained on Mars and Uranus. The sky transparency was virtually constant during each session: it was generally excellent, with the opacity in the line of target ranging from 0.13 to 0.18, except for the observations of LkHα 215 and HK Ori for which we measured 0.33 and 0.45. To improve the quality of the map, we have convolved the images of LkHα 215 and LkHα 233 with a beam of $12''$.

4. Results

4.1. Morphology of the cloud

The ^{13}CO J=1$\rightarrow$0 integrated intensity maps are shown in Figs. 1 and 2. Big differences are found in the morphology of the cloud material around the stars in our sample. While some of them are located at the ^{13}CO integrated intensity peak (PV Cep, ZCMa, LkHα 198, LkHα 234, MWC 1080), others are found at the edges of a ^{13}CO clump (LkHα 215, LkHα 233, BD 61154, MWC 137), and a few in a cavity of the molecular cloud (HD 200775, BD 651637, LkHα 25). The extreme case is HD 52721 toward which we have not detected ^{13}CO J=1$\rightarrow$0 emission down to a limit of 0.3 K kms^{-1}. A similar behavior is observed in the CS J=3$\rightarrow$2 maps. The late-type stars PV Cep and ZCMa, and the early-type stars LkHα 234 and MWC 1080, are found at a peak of the CS J=3$\rightarrow$2 emission. We have detected CS emission toward MWC 137 and LkHα 198 although these stars are not located at the emission peak. We have not detected the CS J=3$\rightarrow$2 line toward HD 200775 (Fuente et al. 1993), BD 651637, HD 52721, LkHα 233, LkHα 215, BD 61154 and LkHα 25. The morphology of the dust emission is in very good agreement with that of the molecular gas. Toward all the stars in which we have detected a CS clump, we have also detected a mm-continuum clump. The stars MWC 137, LkHα 233, and LkHα 215 are located in an extended mm-continuum component which is very

Table 1. List of objects

Spectral types B0-B5

Object	R.A.(1950)	Dec (1950)	Sp. type	Group	d (pc)	Age (yr)	Ref
LkHα234	$21^h41^m57^s.6$	+65°53′07″.1	B5-7	I	1250	$\sim10^5$	1
MWC1080	$23^h15^m14^s.8$	+60°34′19″.2	B0	I	1000	$<10^6$	2
MWC137	$06^h15^m53^s.6$	+15°18′07″.9	B0	I	1300	$<10^6$	2
HD200775	$21^h01^m00^s.0$	+67°58′00″.0	B2.5	I	430	$8\ 10^6$	3
BD651637	$21^h41^m41^s.1$	+65°52′49″.0	B3	III	1250	$5\ 10^6$	2,4
HD52721	$06^h59^m28^s.6$	-11°13′41″.5	B2	III	450	$5\ 10^6$	4

Spectral types B5-A5

Object	R.A.(1950)	Dec (1950)	Sp. type	Group	d (pc)	Age (Myr)	Ref
PVCep	$20^h45^m23^s.5$	+67°46′34″.0	A5	II	500	$1\ 10^5$	1
ZCMa	$07^h01^m22^s.5$	-11°28′36″.0	Bpec	II	1150		
LkHα198	$00^h08^m47^s.4$	+58°33′05″.2	A5	II	600	$1\ 10^5$	1
LkHα215	$06^h29^m56^s.2$	+10°11′51″.0	B7	I	800	$3\ 10^5$	1
LkHα233	$22^h32^m28^s.3$	+40°24′32″.2	A5	II	880	$5\ 10^5$	1
BD61154	$00^h40^m21^s.9$	+61°38′15″.0	B8	I	650	$7\ 10^5$	1,2
LkHα25	$06^h37^m59^s.5$	+09°50′53″.0	B7	II	800	$2\ 10^6$	1
HK Ori	$05^h28^m40^s.1$	+12°07′00″.0	A4	I	450	$5\ 10^6$	1

Ref:(1) Berrilli et al. 1992; (2) Hillenbrand et al. 1992; (3) Hipparcus data;(4) van den Ancker, private communication.

likely associated to the foreground molecular cloud. The cavities observed in the molecular emission around HD 200775 and BD 651637 are also observed in the dust continuum emission (see Table 1 and Figs. 3 and 4). These different morphologies in lines and continuum emission strongly suggest an evolutionary sequence with the stars immersed in a dense clump being less evolved objects than those in a cavity. In this evolutionary scheme, the HAEBE star disperses the dense gas in their surroundings in their evolution to the main sequence. This qualitative description is dependent on the spatial resolution of our observations (the angular size of the beam and the distance to the star). To quantify and characterize this dispersal with a uniform criterion for all the stars, we have used two approachs: i) To calculate the mass in a radius of 0.08 pc around the star; ii) To determine the column density profile of the molecular cloud around the star and investigate the changes in the morphology due to the presence of the HAEBE star.

4.2. Mass around the star

To compare the mass around the stars, it is important to have a uniform spatial scale. We have estimated the masses in a radius of 0.08 pc around the star because this is the linear size of a beam of 24″ (the beam of our ^{13}CO J=1→0 observations) at the distance of MWC 137 (the most distant star). Masses have been calculated using the ^{13}CO, CS and millimeter continuum data. We have estimated the masses from the ^{13}CO J=1→0 and CS J=3→2 data assuming optically thin emission, a characteristic rotation temperature of 30 K, and standard values for the ^{13}CO and CS fractional abundances (2 10^{-6} and 10^{-9} respectively). The uncertainty in the assumed value of the rotation temperature is of a factor of 2 (see e.g. Fuente et al. 1990,1993; Scappini et al. 1994). Since we are in the Rayleigh-Jeans region, this would imply an uncertainty of a factor of 2 in the mass estimates.

The masses from the 1.3mm dust continuum emission have been estimated assuming optically thin emission, an emissivity law κ_λ = 0.02 cm^2 gr^{-1} (λ (mm))$^{-1}$ (Mezger 1990, Beckwith & Sargent 1991, André & Montmerle 1994, Ossenkopf & Henning 1994) and a dust temperature of 30 K. The resulting expression is

$$M(M_\odot) = 1.18 \times 10^{-7} \frac{S_{1.3mm}(Jy) d^2(pc)}{\kappa_{1.3mm}} \quad (1)$$

The largest uncertainties in these estimates comes from the assumed values of $\kappa_{1.3mm}$ and the dust temperature. The emissivity, $\kappa_{1.3mm}$, is dependent on the physical conditions of the studied region. The adopted value, $\kappa_{1.3mm}$ = 0.015 cm^2 gr^{-1} seems to be the most adequate for circumstellar disks (Beckwith & Sargent 1991). However, our 1.3mm continuum maps show that part of the dust emission arise in the foreground molecular cloud. For this extended component, this value could be wrong by a factor of 2 (André & Montmerle 1994). The uncertainty due to the dust temperature is also a factor of 2 (Rayleigh-Jeans region). Thus, the mass estimates based on our 1.3mm data are uncertain by a factor of 4.

Table 2. Observational results

Spectral types B0-B5

Object	Morphology[1]			Mass$_{r=0.08pc}$(M$_\odot$)[2]			α[3]			Type[4]
	^{13}CO	CS	1.3mm	^{13}CO	CS	1.3mm	^{13}CO	CS	1.3mm	
LkHα234	Peak	Peak	Peak	13.6	18.1	16.6	-0.5	-1.4	-1.9	I
MWC1080	Peak	Peak	Off-P	10.5	8.6	3.3	-0.5	-0.9	-1.2	I
MWC137	Off-P	Off-P	Off-P	2.2	1.6	1.4	-0.4	-1.3	-1.3	II
HD200775	Cavity	No	Cavity	1.2			0.7			III
BD651637	Cavity	No	Cavity	0.7	0.9	0.5	0.2	0.0	0.04	III
HD52721	No	No	No							III

Spectral types B5-A5

Object	Morphology[1]			Mass$_{r=0.08pc}$(M$_\odot$)[2]			α[3]			Type[4]
	^{13}CO	CS	1.3mm	^{13}CO	CS	1.3mm	^{13}CO	CS	1.3mm	
PVCep	Peak	Peak	Peak	1.7	1.3	1.0	-0.5	-1.4	-1.4	I
ZCMa	Peak	Peak	Peak	6.8	9.0	6.6	-0.5	-1.7	-2.7	I
LkHα198	Peak	Off-P	Off-P	5.6	1.9	2.3	-0.3	-1.8	-2.6	I
LkHα215	Off-P	No	Off-P	3.9	$\leq$0.9	0.9	-0.2		-0.8	II
LkHα233	Off-P	No	Off-P	3.4	$\leq$0.9	0.5	-0.1	-1.0	-0.9	II
BD61154	Off-P	No		1.0	$\leq$0.3		-0.3			II
LkHα25	Cavity	No	No	1.9	$\leq$0.9	$\leq$0.8	0.8			III
HK Ori			No			$<$0.5				III

[1] Brief description of the morphology of the cloud in ^{13}CO, CS and 1.3 mm continuum emission.*Peak:* the HAEBE star is located at the emission peak; *Off-P:* the star is not located at the emission peak; *Cavity:* The star is located in a cavity *No:* Undetected.
[2] Mass in a radius of 0.08 pc around the star estimated from ^{13}CO data, CS and 1.3mm continuum emission .
[3] Exponent of the density law $N_m \propto r^{\alpha}$ estimated from ^{13}CO, CS and 1.3mm continuum maps.
[4] The new classification proposed in this paper for HAEBE stars.

The masses derived from molecular line and dust continuum emission data are shown in Table 2. When the ^{13}CO J=1$\rightarrow$0 and CS J=3$\rightarrow$2 lines and the continuum emission have been detected toward the star, the masses derived from the different tracers agree within a factor of 3. This is a very good agreement taking into account the large uncertainties involved in these mass estimates. For the sources in which we have not detected CS emission, the masses derived from the different tracers agree within a factor of 7. This larger disagreement is probably due to the fact that in these cases ^{13}CO J=1$\rightarrow$0 emission arise mainly in the foreground molecular cloud. The mean density in the molecular cloud is not high enough to excite the J=3$\rightarrow$2 line of CS. The kinetic gas temperature and the dust temperature in this component could be as low as 10 - 15 K. Furthermore a value of $\kappa_{1.3mm}$ = 0.01 cm^2 gr^{-1} is better suited for these cool regions (Mezger 1990, André & Montmerle 1994, Ossenkopf & Henning 1994).

More important than the agreement between all the tracers for the same source is that we observe the same trend from one source to another. The masses around early-type stars ranges from $>$ 15 M$_\odot$ in the case of LkHα 234 to $\sim$ 0.5 M$_\odot$ in BD 651637. If we ordered the early-type stars by decreasing mass, we obtain the same sequence with all the tracers. Since the ^{13}CO J=1$\rightarrow$0 and CS J=3$\rightarrow$2 lines have different excitation conditions, the agreement between both molecules proves that the changes observed in molecular line emission, and consequently in the masses derived from these data, are not due to different excitation conditions from one region to another. Since ^{13}CO and CS have different chemistries, these changes are not due to chemical differences between the observed clouds either, but to a decrease in the amount of molecular gas around the star. On the other hand, the agreement between the masses derived from the molecular lines and the dust continuum data proves that at the scale considered in this work (0.08 pc around the star), the "molecular gas/dust" ratio is uniform over the sample. This implies that the cavities observed toward a few early-type stars are not the consequence of the photodissociation of the molecular gas by the stellar UV radiation. Since the dust is more resistant than molecules to the effect of UV photons, if the cavities were formed by the stellar UV radiation, the "molecular gas/dust" ratio should be lower in these regions, and consequently the masses derived from dust continuum emission should be larger than the masses derived from molecular lines. These cavities have been formed by the dispersal of the dense gas by the star.

The bipolar morphology of the cavity associated to HD 200775 (see Fuente et al. 1998 and references therein) suggests that the bipolar outflows associated with the first stages of the evolution of these intermediate mass stars can play an important role in the dispersal of this gas.

The same arguments are true for late-type stars. The main difference between early-type and late-type stars is that while the masses derived around early-type are as large as > 15 M$_\odot$, all the masses around late-type stars are $\lesssim 5$ M$_\odot$. The only exception is Z CMa, but this is an unusual FU Orionis star with an uncertain spectral type.

4.3. Column density profile

To estimate the column density profile around the star, we have calculated the mean hydrogen column density in annular regions of 0.08 pc of thickness centered on the star, and fitted the obtained profile with a law $N_m \propto r^\alpha$. For early-type stars we have fitted the column density profile in a radius of 0.40 pc around the star. For late-type stars, our maps do not cover such a large area (see Figs 1,2,3 and 4). In these cases we have fitted the column density in the mapped region. The column densities have been estimated with the assumptions explained in Sect. 4.2. We are aware that the physical conditions of the gas and dust are not uniform over the studied region. In particular, the gas kinetic temperature and the dust temperature are expected to decrease outward the star. But as commented in the previous section, the uncertainties in the column density estimates due to the assumed gas and dust temperatures are at most a factor of 2. As a first approximation, we have considered uniform physical conditions over the whole region and estimate the value of α from ^{13}CO, CS and the millimeter continuum emission. The obtained values are shown in Table 2. As expected, the contrast in the values of α is larger using CS and mm-continuum emission than ^{13}CO. This is because toward the dense clumps the ^{13}CO J=1$\rightarrow$0 line could be optically thick, and far from the star, intense ^{13}CO emission comes from the low density gas (n$\sim$10^3 cm^{-3}) of the foreground molecular cloud. In spite of the differences in the derived absolute values of α, we observe the same trend with all the tracers. The values of α vary from $\alpha < 0$ for the stars immersed in a dense clump to $\alpha > 0$ for the stars located in a cavity of the molecular cloud. For the stars immersed in dense clumps, we obtain $\alpha\sim-0.5$ with ^{13}CO and $\alpha\sim-2.0$ with CS and mm-continuum emission. If we assume that the emitting region is a sphere centered on the star, this will correspond to a density law $n \propto r^{-1.5}$ from ^{13}CO and $n \propto r^{-3.0}$ from CS and dust emission. A density law $n \propto r^{-3.0}$ implies that the dense gas traced by CS and mm-continuum emission is mainly within a radius of 0.08 pc around the star (the first annular region in our calculations). For these stars, the values of α derived from these data are preferred since the ^{13}CO J=1$\rightarrow$0 line could suffer from opacity effects towards the dense clumps. For the stars located in a cavity, we find $\alpha \sim 0-1$ from all the tracers. Intermediate values are found for the stars located in an extended feature. In these cases, the ^{13}CO J=1$\rightarrow$0 line is the best tracer, since the low density gas of the foreground molecular cloud is not detected in the CS J=3$\rightarrow$2 line. In contrast to the behavior of the mass in the surroundings of the star that seems to depend on the stellar mass (see Sect. 4.2), the behavior of α is very similar for early-type and late-type stars. Both, early-type and late-type stars, disperse the dense material of their surroundings in their evolution to the main sequence, and this dispersal changes the morphology of the surrounding cloud. The parameter α seems to establish a more robust criterion to determine the evolutionary stage of HAEBE stars than the surrounding mass.

5. Discussion

5.1. Progressive dispersal of the dense material surrounding the star: a new classification of HAEBE stars

The morphology of the molecular lines and continuum emission around early-type and late-type HAEBE stars seem to vary greatly from one star to another depending on their evolutionary stage. Some stars, that we will call Type I, are located at a mm emission peak and have $\alpha \leq$ -1. This is the case of the late-type stars, PV Cep, ZCMa and LkHα 198, and the early-type stars, LkHα 234 and MWC 1080. Energetic bipolar outflows have been detected towards these stars and are probably in a very early stage of stellar evolution (Cantó et al. 1984, Levreault 1988, Mitchell & Matthews 1994). A second group of stars, Type II, are found immersed in an extended mm clump, but they are not associated with the emission peak. These stars have $\alpha \sim$ -1 to 0 and are probably in a later evolutionary stage. LkHα 233, LkHα 215, BD 61154 and MWC 137 are included in this group. Bipolar outflows have not been detected towards them (Cantó et al. 1984, Levreault 1988). Finally, the stars LkHα 25, HD 200775, BD 651637 and HD52721, are located in a cavity of the parent molecular cloud and have $\alpha > 0$. We will refer to them as Type III. CS and mm-continuum emission have not been detected towards them.

Although the behavior described above is common for both, early-type and late-type HAEBE stars, an important difference exist between them. Early-type stars are much more efficient in the dispersal of the surrounding material than late-type stars. LkHα 234 and BD 651637 constitute a beautiful example of the influence of early-type HAEBE stars on the parent molecular cloud. Both stars have similar mass (around 8 M$_\odot$) and are located in the same cloud. The only difference is their different evolutionary stage. The mass in a radius of 0.08 pc around the star is ≥ 15 M$_\odot$ in LkHα 234 and ≤ 1.0 M$_\odot$ in BD 651637. Therefore in 1 Myr (the age of BD 651637; see Table 1) the mean density in a region of 0.08 pc around the star decreases from $\gtrsim 10^5$ to $< 8\ 10^3$ cm^{-3}. In fact, the integrated intensity map of ^{13}CO shows that BD 651637 has excavated a cavity $\gtrsim$ 1 pc $\times$ 1 pc into the molecular cloud (see Fig. 1) during this time. If we assume that the initial mean density of this region was $\sim 10^5$ cm^{-3}, the star has pushed away ≈ 5600 M$_\odot$ out of a radius of 0.5 pc in 1 Myr, i.e., it has injected energy into the parent cloud at a rate of 0.11 L$_\odot$.

The situation is different for late-type HAEBE stars. The mean density in a region of 0.08 pc around the star decreases

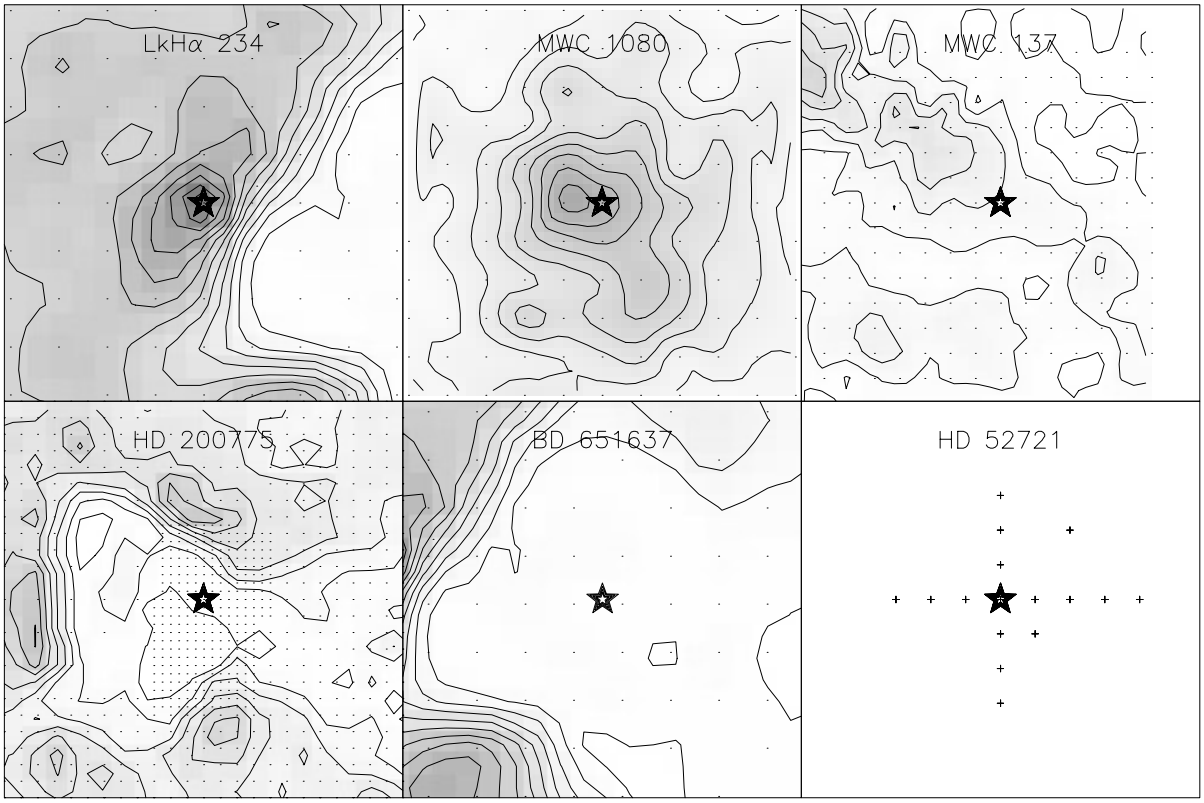

Fig. 1. Integrated intensity maps of the ^{13}CO J=1→0 line around the early-type HAEBE stars of our sample. The size of the box is 1 pc × 1pc for all the objects . Contour levels are 0.3 to 70 by 4 K kms^{-1}. The star position is marked with a star. Crosses indicates the positions observed towards HD52721. The stars are ordered by their evolutionary stage. Note how the amount of cloud mass around the star decreases as the star evolves to the main sequence.

by at most a factor of 5 in their evolution to the main sequence (from 10^4 to a few 10^3 cm^{-3}). The size of the region affected by the star is also smaller than for early-type stars. Taking LkHα 25 as the prototype of an evolved late-type star, we assume that the density in a region of 0.25 pc × 0.25 pc around the star decreases from 10^4 cm^{-3} to 2 10^3 cm^{-3} in their evolution to the main sequence (see Fig. 2). Thus, the star has pushed away 7 M$_\odot$ out of a radius of 0.13 pc in 2 Myrs. The energy has been injected into the parent molecular cloud at a rate of $\sim 10^{-6}$ L$_\odot$, i.e., 5 orders of magnitude less than in the case of an early-type star.

Early-type HAEBE stars are usually born in clusters (see Hillenbrand 1995, Testi et al. 1997). In principle it could be thought that other members of the cluster can contribute to the dispersal of the parent cloud material. However, the early-type HAEBE star is the most massive and evolved member of the cluster and consequently, is expected to have a more important impact on the molecular cloud than the other stars. Note that the energy injected in the parent molecular cloud by an hypothetical late-type HAEBE star of the same cluster would be 5 orders of magnitude lower.

Hillenbrand (1995) carried out a moderate-angular resolution molecular survey toward 17 HAEBE stars (9 of them are also included in our survey) and concluded that there is no relationship between the mass of the HAEBE star and the mass of the cloud or the core morphology. This conclusion is consistent with our results. Both, the morphology of the cloud and the mass around the star, are mainly determined by the evolutionary stage of the star. But when we compare early-type and late-type Type I stars, we find that the masses around early-type stars (M $\sim$ 15 M$_\odot$) are larger than the masses around late-type stars (M $\lesssim$ 5 M$_\odot$). This result is consistent with the idea that a massive core is required to form a high-mass star. A less clear situation is found when we compare Type II and Type III stars because, as commented above, the dispersal of the surrounding material is more efficient for early-type than for late-type stars. Our sample includes only 4 Type I stars. It is important to verify the relationship between the mass of the core and the mass of the star with a wider sample of Type I stars.

We propose an evolutionary sequence for early-type and late-type HAEBE stars, with a progressive dispersion of the material surrounding the star as the star evolves to the main sequence. For this aim, we have ordered the stars according with the parameter α that seems to be the best indicator of the dense material dispersal. For the stars with similar values of α we have taken into account other observational criteria as the amount of mass around the star in absolute value and the existence of a bipolar outflow. The resulting evolutionary sequence is shown in Figs. 1 and 2, and Table 2.

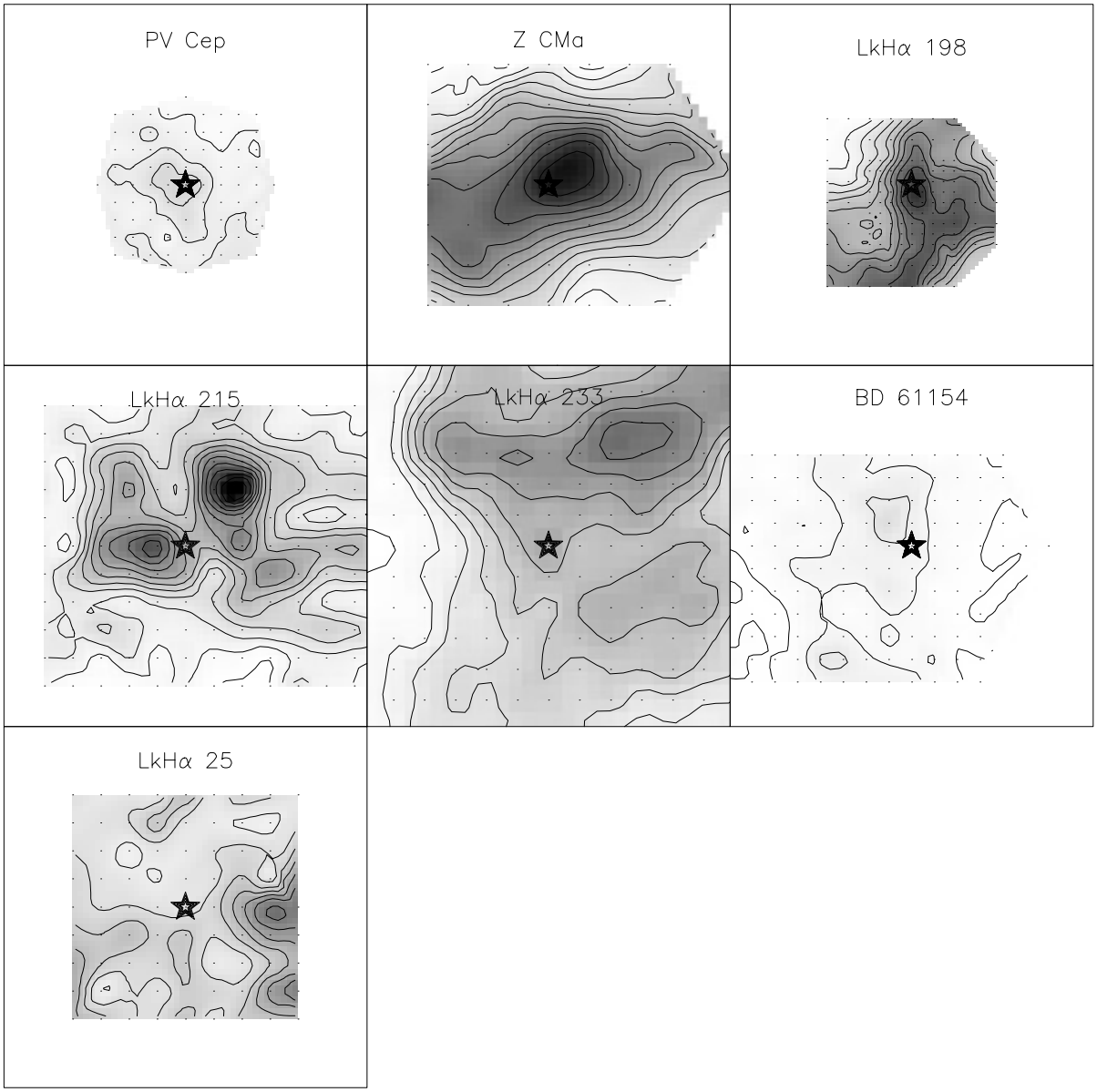

Fig. 2. The same as Fig. 1 for the late-type HAEBE stars of our sample. Contour levels are 0.3 to 70 by 2 K kms^{-1}. Like in Fig. 1 the stars are ordered by their evolutionary stage, and the star indicates the HAEBE star position.

5.2. Correlation between the age of the star and the new classification of HAEBE stars

It is natural to conjecture that the observed dispersal on a large scale of the circumstellar material is correlated with the age of the HAEBE star. In order to check such correlation, we estimate the ages of the stars of our sample from their location in the HR diagram and the use of evolutionary tracks and isochrones from Palla & Stahler (1993). Although uncertainties in the stellar properties are quite large in some cases, we will see that a remarkable trend is indeed found. Fig. 5 shows the distribution of the HAEBE stars in the HR diagram from which we derive the ages listed in Table 1. Luminosities and effective temperatures come from the compilation of Berrilli et al. (1992).

Let us consider first the stars of the late-type group. With the exception of Z CMa, all the other stars have rather well defined properties. The spectral type of Z CMa is very uncertain, varying from B5 to F5. Thus, it is impossible to put the star with some confidence in the HR diagram and we do not consider it in the rest of the discussion. For the other stars, Lk Hα 198 and PV Cep are located very close to the isochrone for 1×10^5 yr and slightly below the birthline obtained with an accretion rate of $\dot{M} = 10^{-5}$ M$_\odot$ yr^{-1}. Lk Hα 215 is located above the isochrone for 5×10^5 yr, Lk Hα233 right onto the isochrone, and BD 61154 below it. Finally, the position of Lk Hα 25 and HK Ori coincides with the isochrones for 2 and 5 Myrs, respectively.

It is more difficult to obtain an accurate age estimate for the early-type stars based on the HR diagram. Protostellar the-

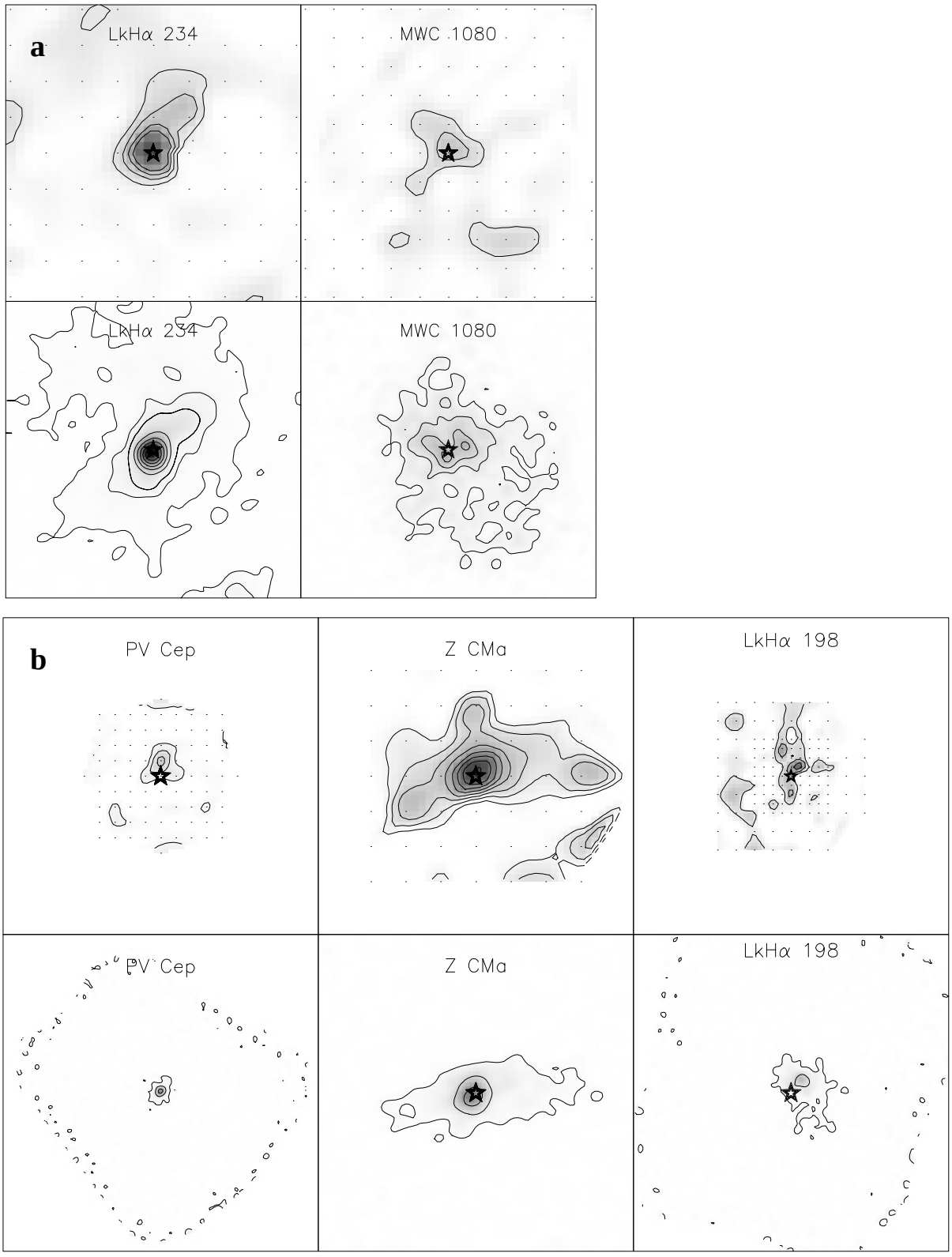

Fig. 3a and b. Integrated intensity maps of the CS J=3→2 line (top panels) and continuum maps at 1.3mm (bottom panels) in a region of 1 pc × 1 pc toward the early-type **(a)** and late-type **(b)** Type I stars. **a** For the CS integrated intensity maps of LKHα 234 and MWC 1080, contour levels are 4 to 10 by 2 K kms^{-1}. For the continuum map of LKHα 234, contour levels are 0.02, 0.07, and 0.11 to 0.68 by 0.11 Jy/ beam. For the MWC 1080 map, contour levels are 0.02 to 0.11 by 0.02 Jy/beam. **b** Contour levels are 1 to 10 by 1 K kms^{-1} for the CS integrated intensity maps and 0.02, 0.11 to 0.34 by 0.11 Jy/beam for the continuum maps. Note that the grey scale is different for each map. For clarity, we have not drawn the star in the continuum map of PV Cep.

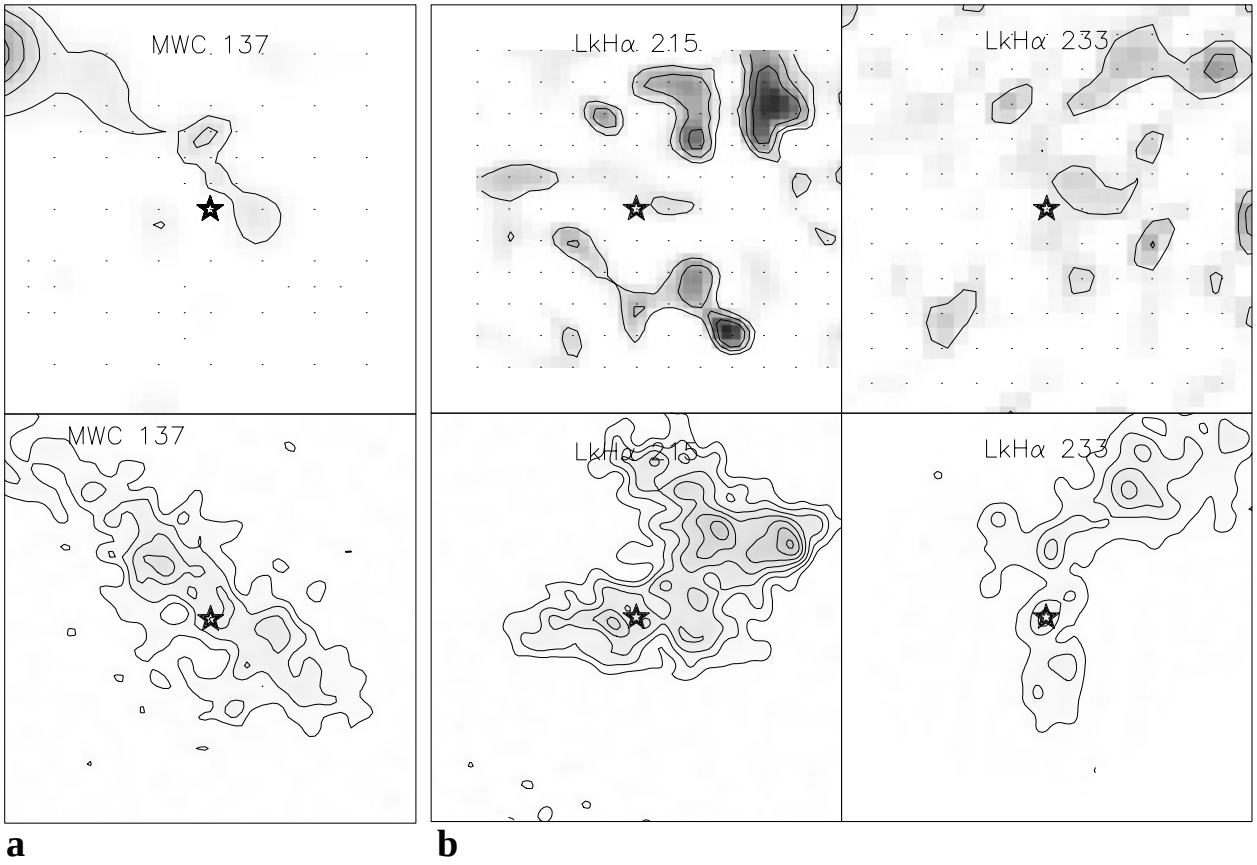

Fig. 4a and b. Integrated intensity maps of the CS J=3→2 line (top panels) and continuum maps at 1.3mm (bottom panels) in a region of 1 pc × 1 pc toward the early-type **a** and late-type **b** Type II stars. **a** Contour levels are 2 to 10 by 1 K kms^{-1} for the CS integrated intensity map, and 0.01 to 0.11 by 0.01 Jy/beam for the 1.3mm continuum map. **b** Contour levels are 1 to 3 by 1 K kms^{-1} for the CS integrated intensity maps and 0.005 to 0.22 by 0.005 Jy/beam for the continuum maps. The 1.3mm continuum maps of LkHα 215 and LkHα 233 have been convolved with a beam of 12″ to improve the signal to noise ratio. Note that in these cases, the star is immersed in an extended component very likely associated with the foreground cloud.

ory predicts that stars more massive than ∼6 M$_\odot$ reach the main-sequence while still accreting matter and therefore completely miss the optically visible phase of pre–main-sequence evolution. Thus, one cannot rely on the evolutionary tracks and isochrones to derive their ages. As can be seen in Fig. 5, five stars out of six of this group fall very close to the ZAMS, above the birthline for $\dot{M} = 10^{-5}$ M$_\odot$ yr^{-1}. The only exception is Lk Hα 234 whose location suggests an age of 1×10^5 yr. Since we cannot use the concept of a PMS phase to assign the ages, we must rely on plausibility arguments only. From an evolutionary viewpoint, early-type stars can be either very young, massive stars still in the accretion phase (e.g. Bernasconi & Maeder 1996) or more mature objects evolving away from the ZAMS. Now, massive protostars are characterized by faster accretion rates than low mass protostars, because of the higher nonthermal support of the parent dense cores. As a reference, in Fig. 5 we have indicated the birthline resulting from an accretion rate of $\dot{M} = 10^{-4}$ M$_\odot$ yr^{-1}. Three stars, HD 200775, BD 651637 and HD 52721, are located below the birthline and we could interpret them as having terminated their main accretion phase and approaching the ZAMS. If these objects were genuine massive PMS stars, then their age would be implausibly small, of order 10^4 yr or less, since the contraction time for stars with mass greater 6 M$_\odot$ is indeed very short. We believe that this possibility is very unlikely. In the alternative explanation of evolved objects, we can estimate their ages using standard main-sequence evolutionary tracks. In Fig. 5 we have shown the tracks from Schaller et al. (1992) limited to the initial 10 Myrs, from which we derive an age of 5 Myrs for BD 651637 and HD 52721 and of 8 Myrs for HD 200775.

The case for MWC 1080 and MWC 137 is less uncertain since in either case of young or evolved objects the age estimate is much less than 1 Myr. In conclusion, we find that three early-type stars (MWC 1080, MWC 137 and LkHα 234) are quite young while the remaining three (BD 651637, HD 52721 and HD 200775) are likely to be evolved objects. According to these results, we have plotted in Fig. 6 the mass in molecular gas surrounding the HAEBE stars as a function of their age. Within the uncertainties of the stellar ages, there exists a clear anticorrelation between the two quantities in both groups of stars, confirming our hypothesis of a progressive dispersal of the parent gas. Thus, we can conclude that the amount of

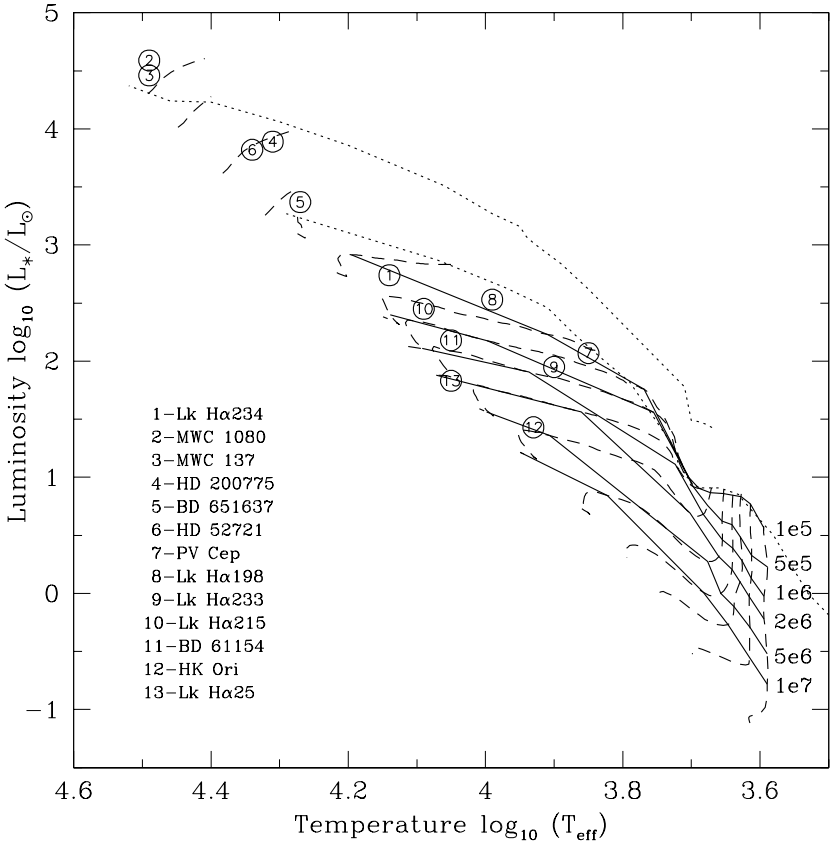

Fig. 5. The location of the HAEBE stars in the HR diagram. The evolutionary tracks (dashed lines) and isochrones (solid lines) for pre-main-sequence evolution are from Palla & Stahler (1993) and for post-main-sequence evolution from Schaller et al. (1992). The tracks refer to the following masses: 0.6, 0.8, 1.0, 1.2, 1.5, 2.0, 2.5, 3.0, 3.5, 4, 5, 6, 7, 9, 12, 15 $M_\odot$. Isochrones from 10^5 to 10^7 yr are labeled at their lower edge. The two dotted lines are the birth-lines computed with $\dot{M} = 10^{-5}$ and 10^{-4} $M_\odot$ yr^{-1}, respectively (Palla & Stahler 1990).

material around a star is mainly determined by its age. It will be very important to verify this initial result on a more statistically significant sample of HAEBE stars.

5.3. Do Hillenbrands' IR Groups represent an evolutionary sequence?

There is no clear correlation between the Hillenbrands' IR Groups and the age of the stars. Following the evolutionary sequence derived from our observations and the stellar age estimates, it seems that early-type HAEBE stars evolve from Group I to Group III in their evolution to the main sequence while late-type stars evolve from Group II to Group I. This difference is not a consequence of a biased star sample but of a different efficiency in the dispersal of the circumstellar dense gas. Hillenbrand et al. (1992) already pointed out that the mean spectral type of the stars of Group I is earlier than that of Group II and concluded that the life time for disks and circumstellar envelopes could be related with the stellar mass. In fact, in the sample of stars studied by Hillenbrand, only two stars with spectral type earlier than B5 belongs to Group II, RCW 34 and R Mon. Interestingly, these stars belong to the rare group of isolated massive stars. This fact suggests that environmental effects could also influence the dispersion of dense material by the star. Group III almost coincides with our Type III and is formed by early-type HAEBE stars that have completely dispersed the dense gas in their surroundings. As commented above, late-type stars are unable to form these large cavities during their PMS phase.

6. Conclusions

We have carried out a systematic study of the environment of 14 HAEBE stars at millimeter wavelengths. Important conclusions are derived from our observations:

- Both, early-type (B0-B5) and late-type (B5-A5) HAEBE stars, disperse the surrounding dense material during their evolution to the main sequence. The efficiency of this dispersal is very different for early-type and late-type stars. While the density in a radius of 0.08 pc around an early-type star decreases by two orders of magnitude during this phase, around a late-type star it decreases by less than an order of magnitude.

- The dispersal of the dense material surrounding the star defines a chronological sequence. Within the groups of early-type and late-type stars, the mass in a radius of 0.08 pc around the star is anticorrelated with the the age of the star. To better characterize the dispersal of dense material around the star we have fitted the column density profile by the exponential law, $N_m \propto r^\alpha$. For early-type as well as for late-type stars, the value of α increases continuously from $\alpha \sim$ -2 to $\alpha > 0$ from the youngest to the oldest star.

-Since the spatial distribution of the dense gas around HAEBE stars seems to be determined by the age of the star, we propose a morphological classification for HAEBE stars. We call Type I stars to those embedded in a dense clump. These stars have $\alpha \sim$ -2, are associated with bipolar outflows and their ages are $\sim 10^5$ yrs. Type III stars are those located in a cavity of the molecular cloud. The values of α are > 0, and their ages are $> 10^6$ yrs.

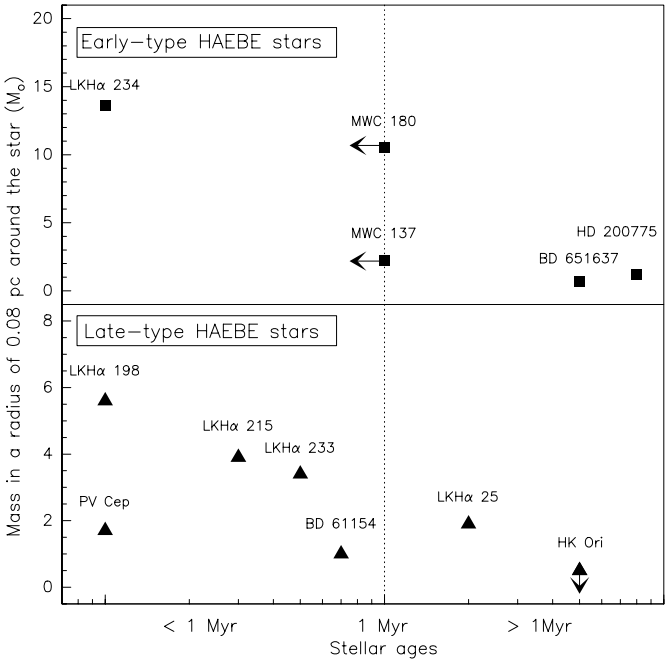

Fig. 6. Plot of the mass in a radius of 0.08 pc around the star against the stellar age for early-type (filled squares) and late-type (filled triangles) HAEBE stars. Note that there exists an anticorrelation between the mass in the surroundings of the star and the stellar age for both early-type and late-type HAEBE stars.

Type II stars are the intermediate case. Although immersed in the bulk of the molecular cloud, they are not located at the emission peak. Furthermore, bipolar outflows are not detected towards them.

Acknowledgements. We are grateful to the technical staff of Pico de Veleta for their support during the observations. This project has been partially supported by the Spanish DGES under grant number PB96-0104, the CNR grant 97.00018.CT02 and the ASI grant ARS 96-66 to the Osservatorio di Arcetri.

References

André P., & Montmerle T., 1994, ApJ 420, 837
Beckwith, S.V.W., & Sargent A.I., 1991, ApJ 381, 250
Bernasconi P.A. & Maeder A., 1996, A & A 307, 829
Berrilli F., Corciulo G., Ingrosso G., Lorenzetti D., Nisini B., Strafella F., 1992, ApJ 398, 254
Cantó J., Rodriguez L.F., Calvet N., Levreault R.M., 1984, ApJ 282, 631
Di Francesco J., Evans N.J. II, Harvey P.M. et al., 1997, ApJ 482, 433
Finkenzeller U. 1985, A & A 151, 340
Finkenzeller U. & Mundt R. 1984, A & AS 272, 249
Fuente A., Martín-Pintado J., Cernicharo J., Bachiller R. 1990, A & A 237, 471
Fuente A., Martín-Pintado J., Cernicharo J., Bachiller R. 1993, A & A 276, 473
Fuente A., Martín-Pintado J., Neri R., Rogers C., Moriarty-Schieven G. 1996, A & A 310, 286
Fuente A., Martín-Pintado J., Neri R., Rodríguez-Franco A., Moriarty-Schieven G. 1998, in preparation
Henning Th., Launhardt R., Steinacker J., Thamm E. 1994, A & A 291, 546
Herbig G.H. 1960, ApJS 4, 337
Herbst W., Holtzman J.A., Phelps B.E. 1982, AJ 87, 1710
Hillenbrand L.A., Strom S.E., Vrba F.J., Keene J. 1992, ApJ 397, 613
Hillenbrand L.A. 1995, PhD University of Massachusets Amherst
Levreault R.M. 1988, ApJS 67, 283
Mannings V. 1994, MNRAS 271, 587
Mezger P. 1990, in Physics and Composition of Interstellar Matter, ed. J. Krelowski & J. Papaj (Torun: Ins. Astron., Nicolaus Copernicus Univ.), 97
Mitchell G.F., Matthews H.E. 1994, ApJ Let 423, L55
Ossenkopf V., Henning Th. 1994, A & A 291, 943
Natta A., Palla F., Butner H.M., Evans N.J.II, Harvey P.M. 1993, ApJ 406, 674
Natta A., Grinin V.P., Mannings V., Ungerechts H. 1997, ApJ 491, 885
Palla F. & Prusti T. 1993, A & A 272, 249
Palla F. & Stahler S.W. 1990, ApJ 360, L47
Palla F. & Stahler S.W. 1993, ApJ 418, 414
Reipurth B., Chini R., Krugel E., Kreysa E., Sievers A. 1993, A & A 273, 221
Scappini F., Palumbo G.G.C., Bruni G., Bergman P. 1994, ApJ 427, 259
Schaller G., Schaerer D., Meynet G., Maeder A. 1992, A & AS 96, 269
Skinner S.L., Brown A., Stewart R.T. 1993, ApJS 87, 217
Testi L., Palla F., Prusti T., Natta A., Maltagliati S. 1997, A & A 320, 159